Antisymmetric and anisotropic exchange in ferromagnetic copper(II) layers

Z. G. Soos, K. T. McGregor,* T. T. P. Cheung, and A. J. Silverstein†
Department of Chemistry, Princeton University, Princeton, New Jersey 08540
(Received 2 May 1977)

The theory of exchange narrowing is extended in systems with large isotropic J_0 to include static spin correlations and antisymmetric exchange. Both contribute to the unusual temperature-dependent, exchange-narrowed EPR linewidth $\Delta H(T)$ in CuX_4^{2-} (X = Cl,Br) salts based on ferromagnetic layers of $s = 1/2$ copper(II) sites. Single-crystal EPR data are presented for $Pt(NH_3)_4CuCl_4$ and for 1-3-propanediammonium-$CuCl_4$ as a function of temperature and crystal orientation. In both salts, $\Delta H(T)$ is shown to be dominated by corrections to J_0, with the antisymmetric exchange larger than the symmetric anisotropic term. Single-crystal EPR provides a novel general approach for finding the magnitude and orientation of the vector $\vec{d}$ for antisymmetric exchange. Antisymmetric contributions to $\Delta H(T)$ are not enhanced by spin diffusion in low-dimensional systems when the paramagnetic sites are at inversion centers. The different role of static spin correlations for symmetric and antisymmetric perturbations accounts without adjustable parameters for the angular anisotropy of $\Delta H(T)$. The residual temperature dependence of the effective exchange frequency is not understood and probably involves various kinds of phonon modulation.

I. INTRODUCTION

Structural[1] and static magnetic[2] studies indicate that various amine salts of copper halides CuX_4^{2-} (X= Cl, Br) crystallize in two-dimensional ferromagnetic layers. All copper (II) sites are in a plane and close to an idealized square-planar geometry, as shown in Fig. 1. Bulk magnetic properties[2] are adequately fit to the isotropic exchange Hamiltonian

$$\mathcal{H}_{ex} = -J_0 \sum_{\langle n,n' \rangle} \vec{S}_n \cdot \vec{S}_{n'}. \tag{1}$$

The sum $\langle n,n' \rangle$ is restricted to nearest-neighbor $s = \frac{1}{2}$ Cu(II) sites in the plane. The interaction $2J_0$ between any $\langle n,n' \rangle$ pair of the extended system can be determined, for example, from static susceptibility measurements. The bridging X^- ions in Fig. 1 provide a superexchange pathway in the plane. These ions are not halfway between the Cu(II) sites and, in addition, are slightly above and below the plane.

It has been amply documented[3] that isotropic exchange interactions J_0 in extended systems produce an "exchange-narrowed" electron-paramagnetic-resonance (EPR) absorption by modulating the local dipolar and hyperfine fields. Extensive recent studies[4,5] of exchange narrowing in low-dimensional spin systems has established that complexes based on S-state ions like Mn(II) provide good experimental realizations of one- and two-dimensional antiferromagnets. Here the dipole-dipole interaction between $s = \frac{5}{2}$ sites is the principal source of broadening, and it often accounts adequately for the observed linewidth. The dipole-dipole interaction can be computed[3] without adjustable parameters whenever the crystal structure and the magnetic moments are known.

Similar analyses of dipolar broadening in Cu(II) crystals, with smaller $s = \frac{1}{2}$ moments, are often an order of magnitude smaller than the observed linewidth. Since Cu(II) has a d^9 electronic configuration and is a D state rather than S-state free ion, it has long been recognized[6,7] that spin-orbit interactions produce additional terms in the spin Hamiltonian. Additional broadening in extended systems is naturally attributed[8] to such corrections to the isotropic exchange. Quite generally, bilinear exchange between sites n and n' can be decomposed[6,7] into an antisymmetric term like $\vec{d} \cdot (\vec{S}_n \times \vec{S}_{n'})$ and a symmetric anisotropic term. The latter has been measured[9] from single-crystal EPR data in several linear antiferromagnetic chains of Cu(II) in which $\vec{d}$ vanishes by symmetry and the exchange correction exceeds the dipolar contribution.

The position of the bridging halide in CuX_4^{2-} salt (Fig. 1) allows both antisymmetric and anisotropic corrections to J_0. In particular, since there is no center of inversion halfway between adjacent Cu(II) sites, the antisymmetric term does not vanish by symmetry.[6] Antisymmetric exchange is relatively

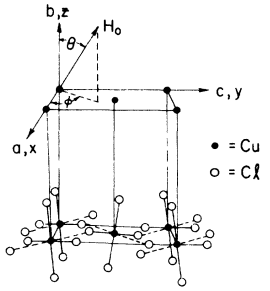

FIG. 1. Schematic representation of the $CuCl_4^{2-}$ layer in the crystalline xy plane and of the polar coordinates θ, ϕ of the magnetic field H_0.

rare and its characterization through the exchange-narrowed EPR line in single crystals has, to the best of our knowledge, not been previously reported.

We have recently shown[10] that local magnetic fields arising from antisymmetric and symmetric perturbations lead to second moments $M_2(J_0/kT)$, and thus to exchange-narrowed linewidths $\Delta H(T)$, with very different temperature dependences which reflect static correlations between the spins. Static-correlations, or short-range order, are particularly important in low-dimensional systems. The temperature dependence of *time* correlation functions requires a more complete understanding of spin dynamics than is presently available.[5] Nevertheless, the ΔH contributions arising from the T dependence of $M_2(J_0/kT)$ can be analyzed from single-crystal EPR data and thus set a limit on the more complicated dynamical contributions.

In this paper, we show that single-crystal EPR data allow the evaluation of the antisymmetric exchange $\vec{d}\cdot\vec{S}_i\times\vec{S}_j$ from measurements in the paramagnetic phase. The two $CuCl_4^{2-}$ crystals studied are Becton's salt, in which the amine is $Pt(NH_3)_4^{2+}$ (PTA), and the 1-3-propanediammonium (PDA) salt. Both are known to crystallize in layers.[11,12] Both are available as small single crystals and neither shows obvious phase transitions on cooling. A single exchange-narrowed EPR line of peak-to-peak width $\Delta H(T)$ is observed in the entire paramagnetic range $\sim 20 < T < 300$ K. The angular dependence of ΔH will be used to estimate both the antisymmetric and anisotropic exchange corrections. Since the anisotropic and antisymmetric contributions to M_2 have different T dependences, fixing these parameters yields a prediction for the T dependence of the angular anisotropy.

The advantages of single-crystal over powder data are illustrated by summarizing previous EPR work.[13-15] The linewidths $\Delta H(T)$ of powdered or polycrystalline samples also decrease monotonically with T, even in the paramagnetic region $kT \gg J_0$, while standard theory[3] predicts a temperature-independent ΔH. The initial evidence[13] for $\vec{d}$ was consequently based on observation that the "infinite-temperature" limit of the extrapolated $\Delta H(T\to 0)$ was still broader than the dipolar contribution. In effect, the antisymmetric exchange provides a single adjustable parameter for a single extrapolated number. Efforts to understand the strong T dependence of ΔH centered on phonon modulation[16] of d, in which the first derivative of the Taylor expansion of $d(R_{ij})$ in the intersite separation $R_{ij}=|R_i-R_j|$ becomes an adjustable parameter, as well as on phonon modulation[17] of the isotropic exchange J_0, which in effect provides a softening of the crystal and leads to a T-dependent $J_0(T)$. The latter approach does not require an antisymmetric exchange, while the former depends on both the antisymmetric exchange and its first derivative. No advantage is taken of the *angular* variation of ΔH which must necessarily arise for a postulated interaction $\vec{d}\cdot\vec{S}_i\times\vec{S}_j$.

We begin in Sec. II with a summary of exchange-narrowing theory, which is extended to include antisymmetric exchange perturbations. The experimental EPR results are collected in Sec. III and are analyzed in Sec. IV in terms of general theory and known structural and magnetic data. Since ferromagnetic layers in $PTACuCl_4$ and in $PDACuCl_4$ do not show low-dimensional anomalies in the EPR linewidth, various limitations to our theoretical approach can be deferred until Sec. V. The single-crystal data suffice for determining the antisymmetric and symmetric exchange corrections in both crystals, but also point to relaxing the rigid-lattice approximation.

II. THEORY OF EXCHANGE NARROWING

Exchange narrowing[3,5] is conveniently treated by a Hamiltonian of the form

$$\mathcal{H}=\mathcal{H}_0+\mathcal{H}'. \tag{2}$$

The zeroth-order Hamiltonian contains the isotropic exchange interaction (1) and the Zeeman interaction

$$\mathcal{H}_0=\mathcal{H}_{ex}+\sum_n \mu_B\vec{H}_0\cdot g\cdot\vec{S}_n. \tag{3}$$

Here, μ_B is the Bohr magneton, $\vec{H}_0$ is the applied static field, and g is the observed g tensor. Since $\mathcal{H}_{ex}$ commutes with any component of the total spin, the spectrum of $\mathcal{H}_0$ is a single δ-function absorption at $\hbar\omega_0=\mu_B|g\cdot\vec{H}_0|$. The perturbation $\mathcal{H}'$ in (2) contains all other terms of the spin Hamiltonian which cause deviations (broadening or shifting) of the sharp resonance at $\hbar\omega_0$. We focus here on the broadening terms of $\mathcal{H}'$.

The observed EPR absorption $I(\omega-\omega_0)$ can formally be written in terms of the relaxation function $\varphi(t)$,

$$I(\omega-\omega_0)=\int_{-\infty}^{\infty} dt\,\varphi(t)\exp i(\omega-\omega_0)t. \tag{4}$$

The relaxation function $\varphi(t)$ is defined[3,5] as

$$\phi(t)=\langle\tilde{M}_+(t)M_-(0)\rangle/\langle M_+M_-\rangle. \tag{5}$$

In (5), M_+, M_- are the transverse magnetization and are proportional to the (+) and (−) components of the total spin, $\langle\ \rangle$ indicates a thermal average, $\tilde{M}_+(t)$ is in the interaction representation ($\hbar=1$),

$$\tilde{M}_+(t)=\exp(-i\mathcal{H}_0t)M_+(t)\exp(i\mathcal{H}_0t), \tag{6}$$

and $M_+(t)$ is in the Heisenberg representation with

respect to $\mathcal{H}_0+\mathcal{H}'$. The thermal average of $\langle M_+M_-\rangle$ is simply related to the intensity of the EPR signal or the static susceptibility $\chi(T)$ via

$$\langle M_+M_-\rangle = 2kT\chi(T) = 2s(s+1)\mu_B^2 g^2\chi(T)/3\chi_C. \quad (7)$$

Thus (7) is a direct measure of spin correlations at any temperature and relates $\chi(T)$ to the Curie-law susceptibility $\chi_C(T)$ of noninteracting spins. When $\mathcal{H}'$ describes Gaussian random processes, Kubo showed[18] that

$$\phi(t) = \exp\left(-\int_0^t (t-\tau)\psi(\tau)\,d\tau\right). \quad (8)$$

The correlation function $\psi(\tau)$ is given by

$$\psi(\tau) = \langle[\tilde{\mathcal{H}}'(\tau), M_+(0)][M_-(0), \mathcal{H}'(0)]\rangle/\langle M_+M_-\rangle, \quad (9)$$

where $\tilde{\mathcal{H}}'(\tau) = \exp(-i\mathcal{H}_0\tau)\mathcal{H}'(0)\exp(i\mathcal{H}_0\tau)$. There are no contributions in (9) from $\mathcal{H}_0$, since $\mathcal{H}_0$ commutes with M_+ or M_-. Thus $\psi(\tau)$ describes the correlations of the local magnetic fields, or of $\mathcal{H}'$ terms. Explicit treatments[3,19] of dipolar or hyperfine contributions to $\mathcal{H}'$ are available.

We focus here on corrections to the isotropic exchange J_0 between nearest-neighbors sites and introduce a general traceless $\mathcal{H}'$

$$\mathcal{H}' = \frac{1}{2}\sum_{\langle nn'\rangle}\sum_{\alpha\beta}\lambda_{n\alpha n'\beta}S_{n\alpha}S_{n\beta}. \quad (10)$$

The $\langle n,n'\rangle$ sum is over nearest neighbors, while the α,β sum is over the components x,y,z. The eight independent $\lambda_{n\alpha n'\beta}$ coefficients in (10) can be decomposed[6,7] into the five components of a traceless symmetric tensor and the three components of an antisymmetric vector. Thus we have

$$\mathcal{H}' = \mathcal{H}'_A + \mathcal{H}'_S = \frac{1}{2}\sum_{\langle nn'\rangle}(\mathcal{H}^S_{nn'} + \mathcal{H}^A_{nn'}), \quad (11)$$

where

$$\mathcal{H}^A_{nn'} = \sum_{\alpha\beta}\lambda^A_{n\alpha n'\beta}S_{n\alpha}S_{n'\beta}, \quad (11a)$$

$$\mathcal{H}^S_{nn'} = \sum_{\alpha\beta}\lambda^S_{n\alpha n'\beta}S_{n\alpha}S_{n\alpha}S_{n'\beta}. \quad (11b)$$

The coefficients $\lambda^A_{n\alpha n'\beta}$ change sign on transposing either α and β or n and n'; hence $\lambda^A_{n\alpha n'\alpha}=0$ for $\alpha=x,y,z$. The coefficients $\lambda^S_{n\alpha n'\beta}$ remain unchanged on transposing α and β or n and n'. The traceless symmetric tensor $\lambda^S_{n\alpha n'\beta}$ transforms like the dipole-dipole interaction and is consequently easily incorporated[9] in standard treatments. Finally, it can generally be shown that symmetric and antisymmetric contributions to $\mathcal{H}'$ are not correlated. Since no cross terms in $\mathcal{H}'_A$ and $\mathcal{H}'_S$ occur in the numerator of (9), $\psi(\tau)$ may be written

$$\psi(\tau) = \psi_A(\tau) + \psi_S(\tau). \quad (12)$$

The relaxation function $\phi(t)$ in (8) is then a product function

$$\phi(t) = \phi_A(t)\phi_S(t). \quad (13)$$

All symmetric and antisymmetric contributions to $\mathcal{H}'$ are therefore computed separately. For example, the second moment M_2 of the resonance line is the amplitude of $\psi(t)$ at $t=0$,

$$M_2(J_0/kT) \equiv \psi(0) = \psi_A(0) + \psi_S(0). \quad (14)$$

A. Evaluation of $M_2(\beta J_0)$

$\mathcal{H}_{ex}$ is, by hypothesis, the largest term in the spin Hamiltonian. All characteristic energies in $\mathcal{H}'$, as well as the Zeeman energy $\hbar\omega_0$, are assumed to be small compared to kT, whereas the isotropic exchange J_0 and kT may be comparable. The usual treatment[3] also has $kT \gg J_0$, when all static spin correlations can be neglected. We generalize[10] to comparable J_0 and kT. Then only $\mathcal{H}_{ex}$ is kept in computing the thermal average of an operator A

$$\langle A\rangle = \mathrm{Tr}\exp(-\beta\mathcal{H}_{ex})A/\mathrm{Tr}\exp(-\beta\mathcal{H}_{ex}), \quad (15)$$

where $\beta=(kT)^{-1}$ and k is the Boltzmann factor. Since (1) is isotropic in spin space, it follows that

$$\langle S_{i\alpha}S_{j\beta}\rangle = \tfrac{1}{3}S(S+1)C(r_{ij},\beta J_0)\delta_{\alpha\beta}, \quad (16)$$

$$\langle S_{i\alpha}\rangle = \langle S_{i\alpha}S_{j\beta}S_{k\gamma}\rangle = 0 \quad (i\neq j\neq k\neq i). \quad (17)$$

The normalized static correlation functions $C(r_{ij},\beta J_0)$ depend only on the distance between the sites and on βJ_0. The assumption that kT is much larger than $\hbar\omega_0$ guarantees that spin polarization is negligible in the paramagnetic phase and leads to the vanishing in (17) of correlations for odd numbers of sites. The analysis for $kT\sim\hbar\omega_0$ becomes considerably more complicated and is not considered here.

The treatment of antisymmetric contributions of $\mathcal{H}'_A$ in (11a) parallels the more familiar analysis[3,5,9,19] of symmetric contributions. We first rewrite $\mathcal{H}^A_{nn'}$ in terms of spin-ladder operators

$$\mathcal{H}^A_{nn'} = G^A_0 + G^A_1 + G^A_{-1}, \quad (18)$$

where the site indices n,n' have been suppressed for simplicity. The secular part, which commutes with $s_{n\varepsilon}+s_{n'\varepsilon}$, is

$$G^A_0 = \tfrac{1}{2}i\lambda^A_{nxn'y}(s^+_n s^-_{n'} - s^-_n s^+_{n'}) \quad (19)$$

and clearly does not vanish in general, in spite of the "nonsecular appearance" of $\vec{d}\cdot\vec{s}_n\times\vec{s}_{n'}$. The nonsecular part G^A_1 for sites n,n' induces ΔM_s changes of 1 and is given by

$$G^A_1 = \tfrac{1}{2}(\lambda^A_{nxn'z} - i\lambda^A_{nyn'z})(S^+_n S_{n'z} - S_{nz}S^+_{n'}). \quad (20)$$

The G^A_{-1} term is the adjoint $(G^A_1)^+$ and induces ΔM_s

changes of -1. There are no $\Delta M_s = \pm 2$ terms.

The definition $M_\alpha = \mu_B g S_\alpha$ in terms of components of the total spin and the explicit expression (19) and (20) for the $\langle nn' \rangle$ components of $\mathcal{H}^A_{nn'}$ are now used to evaluate the $\tau = 0$ commutators in (9). The result is

$$M_2^A(\beta J_0) \equiv \psi_A(0) = \sum_{\langle ij \rangle} \sum_{\langle nm \rangle} [\lambda^A_{ixjy} \lambda^A_{nxmy} \langle S_{iz} S^+_j S_{nz} S^-_m \rangle - \tfrac{1}{4} (\lambda^A_{ixjz} \lambda^A_{nxmz} + \lambda^A_{iyjz} \lambda^A_{nymz}) \langle S^-_i S^+_j S^-_n S^+_m \rangle] / \langle S_+ S_- \rangle . \quad (21)$$

The sums are over nearest-neighbor pairs $\langle ij \rangle$ and $\langle nm \rangle$, and $\langle S_+ S_- \rangle$ is proportional to (7). The high-temperature limit $\beta J_0 \to 0$ consists of retaining only square terms with $i = n$, $j = m$ or $i = m$, $j = n$ in (21). Static correlations for $\beta J_0 > 0$ lead to additional contributions in (21) and for $s = \frac{1}{2}$ sites are amenable to exact analysis[10] for the most important terms in which i, j, n, and m involve only two or three sites. Four-site contributions to (21) are decoupled in the usual manner[5,10] into products of two-spin correlations functions like $C(r_{in}) C(r_{jm})$.

In addition to specializing to $s = \frac{1}{2}$ sites, we also use the structural feature that each site is at a center of inversion, so that whenever $\vec{r}_{ij} = -\vec{r}_{ik}$,

$$\lambda^A_{i\alpha j\beta} = -\lambda^A_{i\alpha k\beta} . \quad (22)$$

This follows from the fact that $\lambda^A_{i\alpha j\beta}$ are components of a vector relating sites i and j. There is a center of inversion at each Cu(II) site in[11] $PTACuCl_4^{2-}$ and[12] $PDACuCl_4^{2-}$, as well as in other CuX_4^{2-} systems.[1] The antisymmetric exchange does not vanish by symmetry because there is no inversion center halfway between nearest-neighbor Cu(II) sites (Fig. 1). The condition (22) not only simplifies the evaluation of $M_2^A(\beta J_0)$, but has important consequences on the spin dynamics, as discussed below.

The computation of $M_2^A(\beta J_0)$ for a square-planar ferromagnetic layer of $s = \frac{1}{2}$ sites at centers of inversion has been discussed in Ref. 10. The result is

$$M_2^A(\beta J_0) = (M^A_{2,0} + M^A_{2,1}) F_A(\beta J_0) \chi_C / \chi(T) . \quad (23)$$

Here, $M^A_{2,0}$ and $M^A_{2,1}$ are the secular and nonsecular contributions, respectively, at high $T(\beta J_0 \to 0)$ and are explicitly given by

$$M^A_{2,0} = \frac{1}{4} \sum_j (\lambda^A_{ixjy})^2 , \qquad M^A_{2,1} = \frac{1}{8} \sum_j [(\lambda^A_{ixjz})^2 + (\lambda^A_{iyjz})^2] . \quad (24)$$

The j sum is over $z = 4$ in the square-planar lattice. The other factors in (23) are the Curie-law susceptibility χ_C, the observed $\chi(T)$ which can be computed from (1), and the factor $F_A(\beta J_0)$ describing the static spin correlation due to $\mathcal{H}_{ex}$. $F_A(\beta J_0)$ is given[10] by

$$F_A(\beta J_0) = 1 - C_1 - 2C_3 + 2C_1^2 + 2C_2^2 + 4C_3^2 \cdots , \quad (25)$$

where C_n is an abbreviation for the nth neighbor $C(r_{ij}, \beta J_0)$ in (16). All $C_n \to 0$ in the high-T limit $\beta J_0 \to 0$. The C_1 and C_3 corrections in (25) are exact and no C_2 terms occur on account of (22). The square terms in (25) are decoupled four-site contributions from (21) and are small[10] for $kT \gtrsim 4J_0$.

The evaluation of $M_2^S(\beta J_0)$ is entirely analogous, except that $\Delta M_s = \pm 2$ nonsecular terms also occur. Once again, conventional high-T results are found for the secular component $M^S_{2,0}$ and nonsecular components $M^S_{2,1} + M^S_{2,2}$

$$M^S_{2,0} = \frac{1}{16} \sum_j [2\lambda^S_{izjz} - \lambda^S_{ixjx} - \lambda^S_{iyjy}]^2 , \quad (26a)$$

$$M^S_{2,1} + M^S_{2,2} = \frac{1}{16} \sum_j \{10(\lambda^S_{ixjz})^2 + 10(\lambda^S_{iyjz})^2 + (\lambda^S_{ixjx} - \lambda^S_{iyjy})^2 + 4(\lambda^S_{ixjy})^2\} . \quad (26b)$$

The static spin correlations due to $\mathcal{H}_{ex}$ now lead to

$$M_2^S(\beta J_0) = (M^S_{2,0} + M^S_{2,1} + M^S_{2,2}) F_S(\beta J_0) \chi_C / \chi(T) . \quad (27)$$

The correlation function $F_S(\beta J_0)$ for symmetric perturbations $\mathcal{H}'$ is[10]

$$F_S(\beta J_0) = 1 + C_1 + 4C_2 + 2C_3 + 2C_1^2 + 6C_2^2 + 8C_2 C_3 + 4C_3^2 \cdots . \quad (28)$$

If both $F_A(\beta J_0)$ and $F_S(\beta J_0)$ are truncated by including spin correlations up the third neighbor, then (25) and (28) are valid[10] down to about $kT \sim 2J_0$. The reduced second moments $F_S \chi_C / \chi(T)$ and $F_A \chi_C / \chi(T)$ are shown in Fig. 2. Their qualitatively different T dependence is particularly noteworthy. The differences in the exact C_1, C_2, and C_3 contributions in (25) and (28) are primarily responsible for the stronger decrease of $F_A(\beta J_0)$ at low temperature. Furthermore, the general nearest-neighbor $\mathcal{H}'$ in (10) for corrections to the isotropic exchange (1) leads, for both symmetric and antisymmetric terms, to a *product* of high-T contributions that depend on the coefficients $\lambda_{i\alpha j\beta}$ and temperature-dependent factors involving only βJ_0. This factorization in (23) and (27) will be extremely convenient for analyzing single-crystal EPR data.

B. Two dimensionality and spin dynamics

While the computation of $M_2(\beta J_0) = \psi(0)$ is somewhat tedious, it is quite straightforward. More

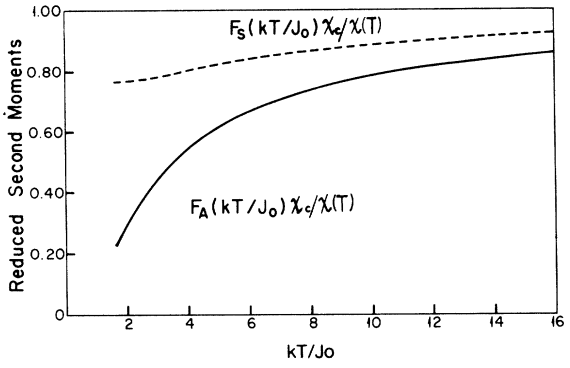

FIG. 2. Effect of static spin correlations in the square planar ferromagnet on the second moment of symmetric [Eq. (27)] and antisymmetric [Eq. (23)] broadening perturbations.

fundamental problems arise with the time dependence of $\psi(\tau)$, which in principle requires a detailed picture of the spin dynamics. Nevertheless, $\psi(\tau)$ is needed to compute the relaxation function $\phi(t)$ and the absorption spectrum $I(\omega-\omega_0)$ in (4). For large J_0, $\psi(\tau)$ decays[3] in times of the order of J_0^{-1}, which may be very fast on the EPR time scale. It is then possible to approximate $\phi(t)$ in (5) by[3,19]

$$\phi_L(t)=\exp\left(-t\int_0^\infty \psi(\tau)\,d\tau\right)=\exp[-t\psi(0)\tau_c]\,. \quad (29)$$

The characteristic time $\tau_c\sim\hbar/J_0$ in (29) measures the decay of $\psi(t)$ and $\omega_e\sim\tau_c^{-1}$ is the corresponding frequency of the exchange modulation. It follows directly from (29) that $I(\omega-\omega_0)$ in (4) has a Lorentzian profile, with half-width of

$$\Gamma=M_2(\beta J_0)\tau_c=\tfrac{1}{2}\sqrt{3}\Delta H\,. \quad (30)$$

The relation between Γ and the peak-to-peak derivative linewidth ΔH, which is usually the observed quantity, is also indicated in (30).

The central idea of exchange narrowing in low-dimensional systems[4,5] is that $\psi(\tau)$ may decay so slowly that the approximation (29) is no longer valid and deviations[5,20] from Lorentzian profiles occur. In particular, at high temperature $\psi(\tau)$ is eventually expected to decay diffusively as $\tau^{-d/2}$, where d is the dimensionality of the exchange-coupled network (1). For $d=1$ or 2, the integral in (29) does not converge and τ_c cannot be defined so simply. Nevertheless, exchange narrowing can be analyzed in terms of non-Lorentzian diffusive profiles, which were first demonstrated[21] in the one-dimensional (1D) antiferromagnet $N(CH_3)_4MnCl_3$ (TMMC), with $s=\frac{5}{2}$ sites, and subsequently in other 1D systems with $s=\frac{1}{2}$ Cu(II) sites[22] and in the 2D antiferromagnet[23] K_2MnF_4.

Even modest exchange between the low-dimensional subsystems may preclude observing non-Lorentzian lines.[24] Then (29) and (30) are again valid, with the proviso[9,23] that secular and long-wavelength ($q=0$) contributions to M_2 may be slightly enhanced. Nonsecular M_2 terms induce $\Delta M_s\neq 0$ transitions and thus have an explicit[3,5] time dependence of $\cos\Delta M_s\omega_0 t$ in (8) which suppresses diffusive behavior at long τ. The greater ΔH found in low-dimensional systems is consequently correlated with the secular parts of $\mathcal{H}'$, which are enhanced on account of the slow decay of $\psi(\tau)$.

We now show that spin diffusion does *not* enhance the secular part of antisymmetric terms in $\mathcal{H}'$ when the sites are at centers of inversion. We introduce Fourier components[5] of the spin by

$$S_{\vec{q}\alpha}=N^{-1/2}\sum_j S_{j\alpha}\exp(i\vec{q}\cdot\vec{r}_j)\,, \quad (31)$$

where the sum is over the square-planar lattice. The wave vectors $\vec{q}=(q_x,q_y)$ are restricted to the first Brillouin zone and satisfy periodic boundary conditions for N sites at spacing a; thus $q_x=2\pi m_x/Na$ and $q_y=2\pi m_y/Na$ are continuous on the interval $(-\pi,\pi)$ in the limit $N\to\infty$. At high T, $\langle S_{q\alpha}(\tau)S_{-q\alpha}\rangle$ obeys a diffusion equation[5] and goes as

$$\langle S_{q\alpha}(\tau)S_{-q\alpha}(0)\rangle=\langle S_{q\alpha}S_{-q\alpha}\rangle e^{-q^2D\tau} \quad (32)$$

at long τ, where D is the diffusion constant. The broadening terms $\mathcal{H}'$ lead to four-spin correlations whose decoupling[5,24] in q space has been carefully discussed for the case of symmetric (dipolar) interactions. A similar treatment of the secular part of the antisymmetric part of $\mathcal{H}'$ yields

$$\psi^A_{S\,EC}(\tau)\sim\sum_{\vec{q}}\left|(\lambda^A_{xy})_{\vec{q}}\right|^2\langle S_{\vec{q}\varepsilon}(\tau)S_{-\vec{q}\varepsilon}\rangle^2\,, \quad (33)$$

where we have neglected several multiplicative factors that do not depend on τ or $\vec{q}$. The Fourier component $(\lambda^A_{xy})_{\vec{q}}$ is given by

$$(\lambda^A_{\alpha\beta})_{\vec{q}}=\sum_j\lambda^A_{i\alpha j\beta}\exp(i\vec{q}\cdot\vec{r}_{ij}) \quad (34)$$

and, as indicated in (24), the secular component is kept in (33). The condition (22) now simplifies (34) to terms that go as $\sin q_x a$ and $\sin q_y a$ on summing over the nearest-neighbors of site i. Symmetric contributions, by contrast, go as $\cos q_x a$. At long time, the $q\sim 0$ components dominate in (32) and it is precisely these components of the secular contributions that are enhanced.[5] The $q\to 0$ antisymmetric contributions are seen from (34) to vanish when there is a center of inversion at site i and consequently are not enhanced. Any enhancement of secular contributions in $PTACuCl_4$

or $PDACuCl_4$ must then reflect symmetric terms in $\mathcal{H}'$.

III. EXPERIMENTAL

Single crystals of $PDACuCl_4$ were grown from saturated aqueous solutions containing stoichiometric amounts of 1-3-propanediammonium-2HCl and $CuCl_2 \cdot 2H_2O$. Analysis: C, 13.01; H, 4.35; Cl, 50.24; Calculated for $C_3H_{12}N_2CuCl_4$: C, 12.80; H, 4.30; Cl, 50.38. Standard Weissenberg and precession x-ray methods were used to identify crystal directions for subsequent EPR rotation axes. The space group and cell constants obtained were identical to those reported by Phelps *et al.*[11] in structural and bulk magnetic studies of $PDACuCl_4$. The orthorhombic space group *Pnma* has cell dimensions $a = 7.20$, $b = 18.25$, and $c = 7.45$ Å. As shown schematically in Fig. 1, the $CuCl_4$ unit has two Cu-Cl bonds of 2.275 Å nearly in the plane and two more at 2.314 Å nearly perpendicular to the plane. The two longer Cu $\cdots$Cl separations nearly in the plane are 2.946 Å. The angle of the Cu–Cl $\cdots$Cu bridge is 165.7° and is presumably the principal superexchange pathway. The layer is puckered by canting $CuCl_4$ units by 1.6° and 9.6° in the a and c directions, respectively. Adjacent $CuCl_4$ layers are canted in alternating directions. These layers are separated, at $\frac{1}{2}b = 9.12$ Å, by layers of protonated-amine counter ions.

Single crystals of $PTACuCl_4$ were kindly provided by J. S. Valentine and were similar to those reported[12] in the preparation and structural determination of Becton's salt. The monoclinic space group $P2_1/c$ has cell constants $a = 7.69$, $b = 7.94$, and $c = 8.06$ Å and $\beta = 91.6°$. The general structure in Fig. 1 now has two short CuCl bonds of 2.302 Å nearly in the plane, two short bonds of 2.271 Å nearly perpendicular to the plane, and two long bonds of 3.257 Å nearly in the plane. The Cu–Cl$\cdots$Cu bridging angle is 167.4°. The interlayer separation of $c = 8.06$ Å is ~1 Å shorter than that of the PDA system. The $Pt(NH_3)_4^{2+}$ counterions reside in the interlayer region.

EPR spectra were collected on a standard Varian E12 spectrometer operating at X-band (~9.5 GHz) microwave frequencies and using 100-kHz modulation of the magnetic field. Crystals were mounted on quartz rods which were affixed to a goniometer capable of 360° rotation. The position of the single exchange-narrowed EPR line and the peak-to-peak derivative linewidth ΔH were measured in the $CuCl_4$ plane and in planes containing the normal to the $CuCl_4$ layer. The temperature dependence of ΔH was measured in the range ~20–300 K for the applied field H_0 parallel and perpendicular to the z axis (Fig. 1). Temperatures were achieved and controlled by an Air Products liquid-helium transfer refrigerator and model OC-20 temperature controller. A calibrated Chromel-Iron alloy thermocouple placed in the sample area was used to measure temperature. Additional data in the range 100–300 K were collected with a Varian V6040 model temperature controller, using liquid N_2 and calibrated by a Chromel-Alumel thermocouple. The accuracy of the temperature measurement is estimated to be ±3 K for both cases.

In addition to xy recorder traces of the EPR spectra, digital data were collected at several temperatures on the $PDACuCl_4$ sample, using a Northern Scientific NS-550 Digital Memory Oscilloscope (DMO). The NS-550 was interfaced to the E-12 so that the spectrometer x-axis drive output (available as 1024 pulses) could scale the 1024 memory boxes of the DMO. A full-scale deflection on the y axis (1 V nominal) was converted into 1000 counts of digita data, with a precision of about ±5 counts (including spectrometer noise.)

A. Results

A single, almost axial g tensor describes the position of the EPR absorption in both $PTACuCl_4$ and $PDACuCl_4$. The z principal axis in Fig. 1 is perpendicular to the plane and has $g_{\parallel} = 2.055 \pm 0.005$ for the PTA crystal and 2.053 ± 0.005 for the PDA crystal. Such values are typical[11,25] for $CuCl_4^{2-}$ complexes and are understood by noting that the $CuCl_4^{2-}$ units based on the short Cu-Cl bonds have a common $g_{\perp}^m$ along the z crystal axis. The PDA crystal has an isotropic $g_{\perp} = 2.169 \pm 0.005$ in the xy crystal plane, to within the ±0.002 accuracy of the experiment. Since the long Cu$\cdots$Cl axes in the layer corresponding to $g_{\parallel}^m$ for a complex are at right angles, the $g_{\perp}$ of the crystal is $\frac{1}{2}(g_{\parallel}^m + g_{\perp}^m)$ for an individual complex.[25] The magnitude of $g_{\perp}$ is in the correct range, since Cu(II) complexes with 4 + 2 coordination have $g_{\parallel}^m - 2 \sim 4(g_{\perp}^m - 2)$. The single EPR absorption in the xy plane is an immediate consequence of exchange coupling between differently oriented complexes, with $J_0 \gg \mu_B |g_{\parallel} - g_{\perp}| H_0$. As shown in Fig. 3, the PTA crystal has a small but quite reproducible anisotropy $|g_x - g_y| = 0.008 \pm 0.002$ in the xy plane. The average value $g_{\perp} = \frac{1}{2}(g_x + g_y) = 2.156 \pm 0.005$ is again typical of such layered $CuCl_4^{2-}$ salts. The 15-G shift between the maximum and minimum position of the absorption in the xy plane correlates with the deviation of the angle $\beta = 91.6°$ of the monoclinic $PTACuCl_4$ structure.[12] An angle $\delta = 91.6°$ between the long Cu$\cdots$Cl axes of the complexes yields, to lowest order in $\Delta g/g$

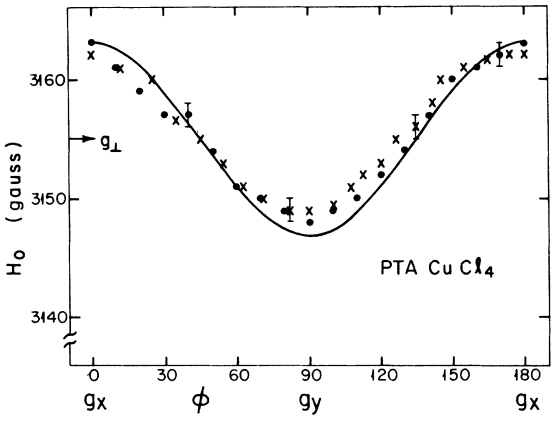

FIG. 3. Position of the exchange-narrowed EPR line in two $PTACuCl_4$ crystals (× and ●) for H_0 in the xy plane. The solid line is a theoretical fit [Eq. (35)] based on structural data.

$$g(\phi) = g_\perp(1 - a \sin 2\phi \cos\delta) \tag{35}$$

for the angular variation of the absorption in the xy plane. The constant a is $2|g_\parallel - g_\perp|/g_\perp$ in terms of the crystal g values. The theoretical curve (35) is plotted in Fig. 3 for $\delta = 91.6$, as obtained from x-ray data, and contains no adjustable parameters.

The temperature dependence of the peak-to-peak derivative linewidth ΔH of the two crystals is shown in Fig. 4 for an applied field along the z axis and in the xy plane. The rapid increase below 20 K is an indication of incipient spin ordering and will not be discussed here. Above this region, both complexes have symmetric Lorentzian absorptions. Within the experimental error of ±1 G, an isotropic $\Delta H_\perp(T)$ was found in the xy plane. Both systems show in Fig. 4 a greater

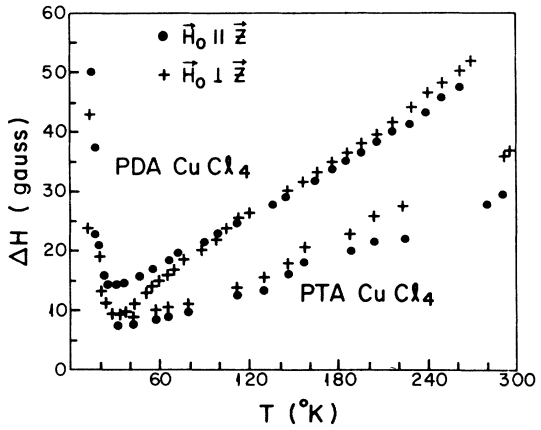

FIG. 4. Temperature dependence of the linewidth ΔH in $PTACuCl_4$ and $PDACuCl_4$ for H_0 in the copper plane (perpendicular to z) and along the normal to the plane (parallel to z). Both crystals show rapidly increasing ΔH below about 20 K.

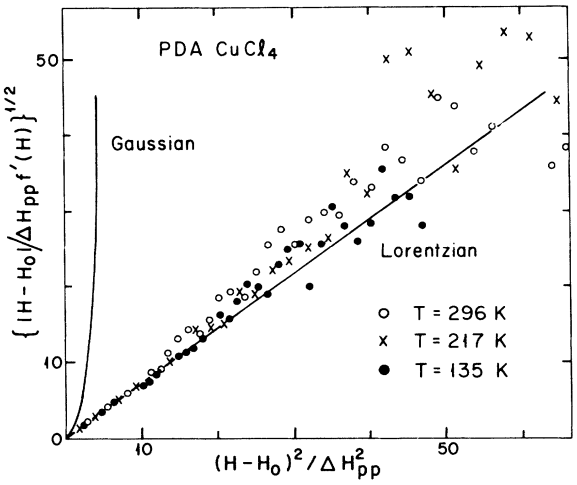

FIG. 5. Analysis of the shape of the EPR absorption in $PDACuCl_4$ at three temperatures. The digital data indicate a Lorentzian absorption within experimental error.

variation in $\Delta H_\perp(T)$ than in $\Delta H_\parallel(T)$.

Since the $PDACuCl_4$ crystal has the greater interlayer separation by about 1 Å, it was expected to provide a better test for possible deviations from a Lorentzian profile. Digital data were collected at several temperatures and plotted in Fig. 5 in the usual manner[5,21-23] to display possible deviations from Lorentzian behavior. While some non-Lorentzian behavior might be argued at 296 K, the data in Fig. 5 can be characterized as Lorentzian within the accuracy of the measurement. As has already been discussed, deviations are by no means easy to measure in two-dimensional systems. Our subsequent analysis is based on Lorentzian profiles, with peak-to-peak linewidths of ΔH.

As can be seen from Fig. 4, the PTA system has a far larger anisotropy in ΔH than the PDA crystal. The angular anisotropy $\Delta H(\theta)$ for $PTACuCl_4$ at room temperature is shown in Fig.

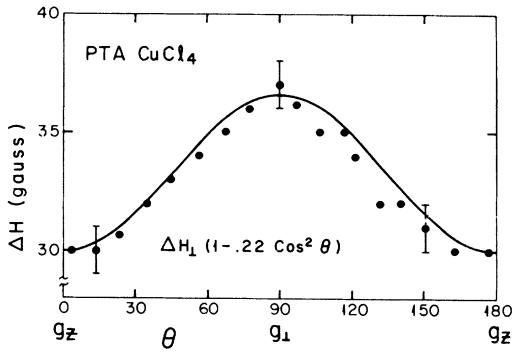

FIG. 6. Angular variation of the $PTACuCl_4$ linewidth at 300 K on rotating the crystal from H_0 normal to the copper plane ($\theta = 0$) to H_0 in the copper plane ($\theta = \frac{1}{2}\pi$).

6. The ϕ variable can be suppressed, since ΔH is isotropic in the xy plane. The rather modest angular anisotropy shown by these crystals tends to limit the accuracy of parameters derived from single-crystal EPR data. Nevertheless, the general features of an axially symmetric $\Delta H(\theta)$ will suffice to identify the broadening contributions in $\mathcal{H}'$.

IV. LINEWIDTH ANALYSIS

The single exchange-narrowed Lorentzian EPR absorption of either $PTACuCl_4$ or $PDACuCl_4$ indicates that (30) is applicable in the form

$$\Delta H = 2M_2(\beta J_0)/\sqrt{3}\,\omega_{eff}. \tag{36}$$

The computation of $M_2(\beta J_0)$ was discussed in Sec. IIA for various broadening contributions to $\mathcal{H}'$. Since the spin dynamics are not fully understood, we write $\tau_c^{-1} = \omega_{eff}$ and treat ω_{eff} as a parameter with an unknown temperature dependence. At high temperature, ω_{eff} is of the order of $J_0/\hbar \sim 2\times 10^5$ G for both $PDACuCl_4$ and $PTACuCl_4$. Static susceptibility data[11] yield $J_0/k_B = 15.4$ K in the former; the value $J_0/k_B \sim 18$ K found[2] in several other $CuCl_4^{2-}$ salts is used for the latter until an accurate determination is made.

Such large values of $\omega_{eff} \gtrsim 2\times 10^5$ G clearly eliminate all broadening contributions $\mathcal{H}'$ whose second moments are less than 10^5 G^2. For example, the dipole-dipole interaction between $s=\frac{1}{2}, g\sim 2$ moments separated by more than 5 Å yields $M_2 \sim 10^5$ G^2, which is at most comparable to the ±1 G experimental error in the measurement of ΔH. Hyperfine constants for Cu(II) sites with 4+2 coordination are about $A_\parallel \sim 200$ G and $A_\perp \sim 20$ G; the resulting $M_2 \sim A_\parallel^2$ also makes a negligible linewidth contribution. The g-tensor inequivalence of the $CuCl_4^{2-}$ complexes in the xy plane leads to an M_2 contribution that goes as $\cos^2 2\phi$ for H_0 in the plane. The amplitude of $\sim(g_\parallel - g_\perp)^2\mu_B^2 H_0^2/2\bar{g})^2$ is negligible at X band ($H_0 \sim 3.3$ kG) and is on the order of 10^5 G^2 at Q band ($H_0 \sim 12$ kG). The Q-band ΔH of $PTACuCl_4$ is at most 1–2 wider[26] and does not show a $\cos^2 2\phi$ angular dependence, thus ruling out this broadening contribution even at higher applied fields.

Essentially the entire ΔH of both $PTACuCl_4$ and $PDACuCl_4$ must consequently reflect other broadening mechanisms. In view of the large J_0 and the known[6,7] corrections to isotropic exchange arising from spin-orbit coupling, it is natural to consider antisymmetric and symmetric anisotropic exchange contributions to ΔH. Both lead to nearest-neighbor interactions of the kind analyzed in Sec. II.

We begin with the more familiar[6,9] symmetric anisotropic term, the D tensor. Its magnitude[6] is of the order of $(\Delta g/g)^2 J_0 \sim 10^3 G$ and its principal axes coincide with those of the g tensor. It dominates[9,27] ΔH when J_0 is large. For the idealized geometry (Fig. 1) of exchange between $CuCl_4^{2-}$ complexes with orthogonal long Cu···Cl axes in the xy plane, it can readily be shown[28] that the crystal D tensor is again axial, with the symmetry axis along $\hat{z}$. The principal axes of the D and g tensors of the crystal still coincide. The latter are known from the position of the resonance. The coordinates in Fig. 1 may then be used for the symmetric anisotropic interaction,[9]

$$\begin{aligned}\mathcal{H}'_S = \frac{1}{2}\sum_{\langle nn'\rangle}\frac{D}{3}\{&(3\cos^2\theta - 1)[s_{n\hat{z}}s_{n'\hat{z}} - \tfrac{1}{4}(s_n^+ s_{n'}^- + s_n^- s_{n'}^+)]\\ &+ 3\sin\theta\cos\theta\tfrac{1}{2}(s_{n\hat{z}}s_{n'}^+ + s_n^+ s_{n'\hat{z}} + \text{H.c.})\\ &+ 3\sin^2\theta\tfrac{1}{4}(s_n^+ s_{n'}^+ + \text{H.c.})\}.\end{aligned} \tag{37}$$

Here H.c. indicates the Hermitian conjugate, $\langle n,n'\rangle$ is restricted to nearest neighbors in the plane, and θ is the azimuthal angle of the field H_0. The angular dependence of $\mathcal{H}'_S$ is known in advance from the principal axes of the g tensor. The magnitude of D is the only adjustable parameter. The coefficients $\lambda^S_{n\alpha n'\beta}$ of (11b) are explicitly related in Table I to $\mathcal{H}'_S$. Then (26a) and (26b) give the secular and nonsecular contributions to $M_2^S(\beta J_0)$. For the square-planar lattice ($z=4$) we obtain

$$M_2^S(0) = \tfrac{1}{8}zD^2(1+\cos^2\theta) \tag{38}$$

for the entire (secular and nonsecular) broadening due to (37). The temperature dependence of $M_2^S(\beta J_0)$ is then given by (27).

The antisymmetric correction $\vec{d}\cdot\vec{s}_i\times\vec{s}_j$ has not been characterized quantitatively in these systems. Although d is potentially as large as $(\Delta g/g)J_0$, it vanishes by symmetry when the two ions have a center of inversion midway between them.[6] Figure 7 shows schematically the local Cu···Cl–Cu pathway. If the Cl were in the plane, by tilting the octahedra by α, then there would be a C_2 axis and $\vec{d}$ would be along the Cu-Cu separation. If, in addition, the Cl were midway between the coppers (a shift of ~0.5 Å) then d would vanish on account of the center of inversion. Strictly speaking, the actual structure places no restriction on either the orientation or magnitude of $\vec{d}$. Nevertheless, it is likely that d is along the Cu-Cu direction and that it is far smaller than its possible maximum of order $(\Delta g/g)J_0$.

The experimentally observed ΔH in both crystals were axially symmetric about $\hat{z}$. Since the symmetric anisotropic contribution (38) is also axial, there are essentially only two choices for the direction of $\vec{d}$. Either $\vec{d}$ is along $\hat{z}$ for all pairs or $\vec{d}$ is along the Cu-Cu separations, which leads to equal numbers of orthogonal $\vec{d}$ vectors in the xy

TABLE I. Coefficients for anistropic (37) and antisymmetric (39) exchange for a square-planar layer, with the polar angles (θ, ϕ) of H_0 indicated in Fig. 1.

Symmetric anisotropic exchange [Eq. (37)]	$3\lambda^S_{izjz} = D(3\cos^2\theta - 1)$
	$2\lambda^S_{ixjx} = -\lambda_{izjz} + D\sin^2\theta$
	$2\lambda^S_{iyjy} = -\lambda_{izjz} - D\sin^2\theta$
	$\lambda^S_{ixjz} = \lambda^S_{izjx} = D\cos\theta\sin\theta$
	$\lambda^S_{iyjz} = \lambda^S_{izjy} = \lambda^S_{ixjy} = \lambda^S_{iyjx} = 0$
Antisymmetric exchange [Eq. (39)]	$\vec{d} \parallel \hat{x}$: $\lambda^A_{ixjy} = d\sin\theta\cos\phi$
	$(\lambda^A_{ixjz})^2 + (\lambda^A_{iyjz})^2 = d^2(1 - \sin^2\theta\cos^2\phi)$
	$\vec{d} \parallel \hat{y}$: $\lambda^A_{ixjy} = d\sin\theta\sin\phi$
	$(\lambda^A_{ixjz})^2 + (\lambda^A_{iyjz})^2 = d^2(1 - \sin^2\theta\sin^2\phi)$

plane. The antisymmetric contribution to $\mathcal{H}'$ is

$$\mathcal{H}'_A = \frac{1}{2}\sum_{\langle nn'\rangle} \vec{d}_{nn'} \cdot \vec{s}_n \times \vec{s}_{n'} \tag{39}$$

for nearest neighbors n, n' in the plane. The $\lambda^A_{n\alpha n'\beta}$ coefficients of (11a) are related in Table I to (39) for $\vec{d} \parallel \hat{x}$ and for $\vec{d} \parallel \hat{y}$. The secular contribution (19) and the nonsecular contribution (20) to the second moment (21) is given, at high temperature, by (24) to be

$$M_2^A(0) = \tfrac{1}{16} z d^2 (2 + \sin^2\theta). \tag{40}$$

We have again used $z = 4$ for the square-planar lattice and have also used the fact that each Cu(II) has two neighbors along $\hat{x}$ and two along $\hat{y}$. It is evident that (40) preserves the axial symmetry of ΔH and gives $\Delta H_\perp > \Delta H_\parallel$ in (36). The alternate choice of $\vec{d} \parallel \hat{z}$ for all complexes leads to the $1 + \cos^2\theta$ angular dependence of $M_2(0)$ and thus always predicts $\Delta H_\parallel$ to be larger than $\Delta H_\perp$, in disagreement with experiment. The experimental data at once place the orthogonal $\vec{d}$ vectors in the xy plane, but without direct evidence for the choice (39) of $\vec{d}$ along the Cu-Cu directions.

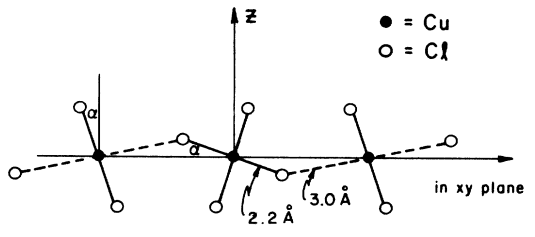

FIG. 7. Schematic representation of the $CuCl_4^{2-}$ octahedra in the xy plane. Each Cu has two additional short Cu-Cl bonds above and below the plane of the paper.

A. Evaluation of parameters

We showed that dipolar, hyperfine, and g-tensor contributions to M_2 were negligible. The remaining antisymmetric exchange (39) and symmetric anisotropic exchange (37) yield an axial $M_2(\theta, T)$,

$$M_2(\theta, T) = \{M_2^A(\theta)F_A(kT/J_0) + M_2^S(\theta)F_S(kT/J_0)\}\chi_C/\chi(T). \tag{41}$$

Here $M_2^A(\theta)$ and $M_2^S(\theta)$ are the high-temperature second moments (40) and (38), respectively, and involve the adjustable parameters d and D. The temperature-dependent factors $F_A(kT/J_0)$ and $F_S(kT/J_0)$ for a square-planar Heisenberg ferromagnet are given in (25) and (28), respectively, and are plotted in Fig. 2. We showed in Sec. II B that the secular components of the antisymmetric exchange broadening are not enhanced by low-dimensional effects in systems with local moments at centers of inversion. Possible enhancements of the secular components of $\mathcal{H}'_S$ would lead to deviations from Lorentzian profiles and to enhanced $(3\cos^2\theta - 1)^2$ angular behavior.[9,23] The digital data in Fig. 5 and the angular data in Fig. 6 show neither deviations from Lorentzian shape nor minima at $3\cos^2\theta = 1$. Thus we use the unenhanced results $M_2^A(\theta)$ and $M_2^S(\theta)$ in (41). Finally, the possible angular variation of the effective modulation ω_{eff} can usually be neglected.[19] Exceptions may occur in low-dimensional systems with strong $q = 0$ enhancement, as shown in Ref. 23, where ΔH and M_2 can have different angular dependences. According to the approximation (36), this would yield an ω_{eff} that depends on angle. However, we have shown that the $q = 0$ component of the antisymmetric exchange contribution vanishes and have no evidence for $q = 0$ enhancement of the smaller symmetric term. Thus ω_{eff} is expected to be approximately isotropic.

Substitution of (41) into (36) then shows that

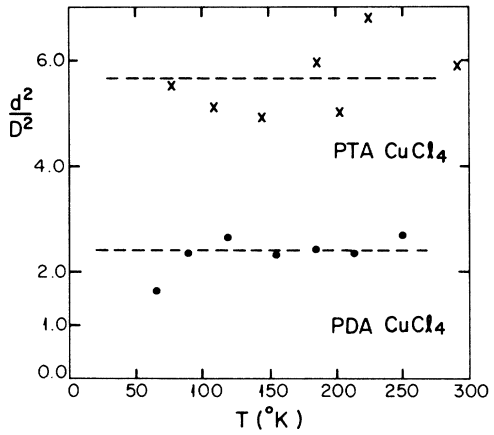

FIG. 8. Evaluation of the ratio of antisymmetric (d) and symmetric anisotropic (D) exchange in $PTACuCl_4$ and $PDACuCl_4$, based in Eq. (42). There are no adjustable parameters.

$\Delta H(\theta, T)$ goes as $1 + c\cos^2\theta$ at any T, with $c > 0$ when $\mathcal{H}'_S$ dominates and $c < 0$ when $\mathcal{H}'_A$ dominates. The 300 K data for $PTACuCl_4$ are fit in Fig. 6 with $c = -0.22$. A high T, both F_A and F_S are close to unity (Fig. 2) and the ratio $\Delta H(0) \equiv \Delta H_{\parallel}$ and $\Delta H(\frac{1}{2}\pi) \equiv \Delta H_{\perp}$ yields, from (38) and (40)

$$\Delta H_{\parallel}/\Delta H_{\perp} \approx 1 + c = (4D^2 + 2d^2)/(2D^2 + 3d^2). \tag{41}$$

The experimental value of $c \sim -0.22$ for $PTA\text{-}CuCl_4$ indicates that $(d/D)^2$ is approximately 6. At 300 K, $\Delta H_{\perp}$ is slightly larger than $\Delta H_{\parallel}$ for $PDACuCl_4$ also (Fig. 4); this indicates $(d/D)^2 > 1$ in that system as well.

By considering the ratio $\Delta H_{\parallel}/\Delta H_{\perp}$, we may eliminate the (unknown) temperature dependence of ω_{eff} in (36). A slight rearrangement of (40), (38), (41), and (36) yields

$$\left(\frac{d}{D}\right)^2 = 2\frac{F_S(\beta J_0)(2\Delta H_{\perp} - \Delta H_{\parallel})}{F_A(\beta J_0)(3\Delta H_{\parallel} - 2\Delta H_{\perp})}. \tag{42}$$

The right-hand side of (42) contains the observed linewidths (Fig. 4) and the calculated static correlations (Fig. 2) for symmetric and antisymmetric perturbations. Static magnetic data give $\beta J_0 = 15.4/T$ for the PDA system and about $18/T$ for PTA. Thus (42) allows an evaluation of d/D without any adjustable parameters and without having to specify the temperature dependence of ω_{eff}. Figure 8 shows that $(d/D)^2$ is reasonably constant at 5.6 ± 1 for $PTACuCl_4$ and at 2.2 ± 0.6 for $PDACuCl_4$ for $kT > 3J_0 \sim 50$ K. The low-temperature increase of ΔH in Fig. 4 is, as already mentioned, related to the incipient transition to an ordered state. The no-parameter fit in Fig. 8 illustrates the self-consistency of the assumed broadening mechanisms and of the static spin correlations leading to F_S and F_A.

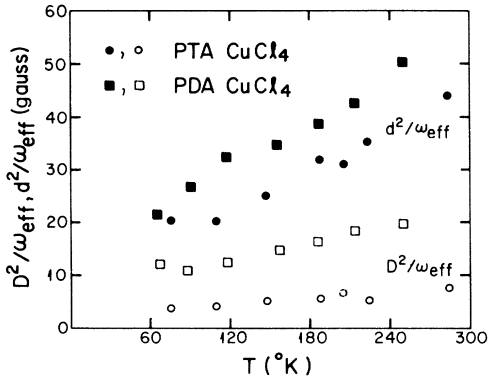

FIG. 9. Residual temperature dependence of D^2/ω_{eff} [Eq. (43a)] and d^2/ω_{eff} [Eq. (43b)] in $PTACuCl_4$ and $PDACuCl_4$.

Thus d and D are comparable in these systems. The latter can often be estimated from $(\Delta g/g)^2 J_0$, which then provides an estimate for d as well. As expected from the near occurrence of a C_2 axis (Fig. 7) connecting adjacent Cu(II) sites, the antisymmetric exchange is in the layer and is far less than $(\Delta g/g)J_0$. In addition, the more strongly T-dependent antisymmetric contribution in the layer accounts for the greater slope of $\Delta H_{\perp}(T)$ than $\Delta H_{\parallel}(T)$ in Fig. 4 for both systems.

The temperature dependence, if any, of $\omega_{\text{eff}}(T)$ can also be measured from the data in Fig. 4 and is required for accurate determinations of D or d. Rearranging (36), (38), (40), and (41) yields

$$\frac{D^2}{\omega_{\text{eff}}} = \frac{\sqrt{3}\,(3\Delta H_{\parallel} - 2\Delta H_{\perp})\chi(T)}{4F_S(\beta J_0)\chi_C}, \tag{43a}$$

$$\frac{d^2}{\omega_{\text{eff}}} = \frac{\sqrt{3}\,(2\Delta H_{\perp} - \Delta H_{\parallel})\chi(T)}{2F_A(\beta J_0)\chi_C}. \tag{43b}$$

Figure 9 shows that both D^2/ω_{eff} and d^2/ω_{eff} contain significant temperature dependence, arising from some combination of $\omega_{\text{eff}}(T)$ or $D(T)$ or $d(T)$. Any of these quantities have temperature dependences once lattice vibrations and thermal expansion of the crystal are considered. In effect, the static correlations F_A and F_S account without additional parameters for about half of the temperature dependence of ΔH in Fig. 4 and show that d/D is essentially constant. The remaining temperature dependence of ΔH does require additional parameters, for example, those arising from a nonrigid lattice.

V. DISCUSSION

The present work relies implicitly on recent demonstrations[5] that the estimate (30) for the exchange-narrowed linewidth ΔH can be made quantitative in spin systems containing only dipolar or hyperfine contributions to $\mathcal{H}'$ when high-tempera-

ture spin dynamics are applicable. In favorable cases no adjustable parameters are needed, since dipolar contributions to $\mathcal{H}'$ can be computed from the crystal structure and J_0 is known from static data. The fact that complete agreement between calculated and observed linewidths is nevertheless rare points to additional contributions to $\mathcal{H}'$ and/or to more complicated dynamics at room temperature and below. It is easy to show that $s=\frac{1}{2}$ sites in $CuCl_4^{2-}$ sheets have insufficient dipolar, hyperfine, or anisotropic g-tensor coupling to produce $\Delta H \sim 50$ G for $J_0/\hbar \sim 2\times 10^5$ G. The method of analyzing the dominant antisymmetric and symmetric anisotropic exchange corrections then involved usual single-crystal techniques. Similar methods can be used whenever ΔH is dominated by an $\mathcal{H}'$ term whose amplitude and angular dependence are to be found.

The present systems offer several constrasts to dipolar broadening in antiferromagnetic K_2MnF_4 layers.[5,23] There, the occurrence of orthogonal Mn-Mn vectors in the plane, in contrast to the common θ dependence of the symmetric anisotropic contribution (37), led to a different angular dependence for the secular part of M_2 and its $q=0$ component. Thus the angular dependence of ω_{eff} observed in K_2MnF_4 would not be expected even for the symmetric exchange broadening in these $CuCl_4$ layers. The larger antisymmetric term, which vanishes in K_2MnF_4, has no $q=0$ component to be enhanced and thus also has ω_{eff} essentially independent of angle.

Another important advantage of single-crystal work is the possibility of eliminating unknown parameters like $\omega_{eff}(T)$ which are essentially independent of orientation. This was illustrated for the ratio d/D (Fig. 8) of these two $CuCl_4^{2-}$ systems. The remaining temperature dependences in Fig. 9 then offer tests for improved theories. For example, spin correlations in low-dimensional systems can also be expected to enter in $\omega_{eff}(T)$, although the precise manner is not yet known. This approach does not go beyond the rigid-lattice approximation of $\mathcal{H}_0+\mathcal{H}'$. Alternately, postulating a nonrigid lattice introduces a variety of relaxation processes whose coupling constants are adjusted to fit available experimental data.

Zaspel and Drumheller[17] have considered the thermal expansion of the $CuCl_4^{2-}$ lattice as a way of decreasing J_0 with increasing temperature. This clearly provides a uniform scaling of $\Delta H(\theta,\phi)$ in (36) through a common $\omega_{eff}(T)\sim J_0(T)/\hbar$. A surprisingly soft lattice was postulated to account for the *entire* variation of $\Delta H(T)$. The different behavior of $\Delta H_{\parallel}(T)$ and $\Delta H_{\perp}(T)$ in Fig. 4 immediately rules out this model as the only source of T dependence. About half of the $\Delta H(T)$ variation are consistent with the static correlations $F_A(kT/J_0)$ and $F_S(kT/J_0)$, which involve no adjustable parameters. The residual temperature dependences in Fig. 9 could be assigned to a thermal expansion $J_0(T)$ of a stiffer lattice. The comparable fractional changes of d^2/ω_{eff} and D^2/ω_{eff} in Fig. 9 for both crystals is consistent with a single $J_0(T)$ in these closely related structures. A change in J_0 by less than a factor of 2 between 60 and 300 K would be required in such a model. We are not aware of data that either strongly supports or rules out such an interpretation.

Seehra and Castner[16] have emphasized that phonon modulation of $\vec{d}$ quite generally yields a $\Delta H(T)$ proportional to T, but their estimate of d as $(\Delta g/g)(\partial J_0/\partial R)$ is not convincing. Consider, for example, a torsional oscillation of the complexes in Fig. 7 in which the angle α changes to produce a C_2 axis. Such a low-energy, and thus easily excited, mode affects the orientation of $\vec{d}$ without changing R. The main point[16] is that phonon modulation of d may be particularly important. The data in Fig. 8 show that d/D is constant and comparable in $PTACuCl_4$ and $PDACuCl_4$. Thus d is far smaller here than its theoretical maximum of $(\Delta g/g)J_0$. The residual T dependences of d^2/ω_{eff} and D^2/ω_{eff} in Fig. 9 clearly show that, for fixed ω_{eff}, d^2 and D^2 have comparable temperature dependences. While the phonon modulation of d is qualitatively consistent with the greater variation $\Delta H_{\perp}(T)$ than $\Delta H_{\parallel}(T)$, it is clearly insufficient (even with an adjustable parameter) to account for the single-crystal data. In our opinion, the strongest evidence for phonon modulation is the behavior of $\Delta H(T)$ at high T, where static correlations are less important, and such increases are also observed[9] in systems in which $\vec{d}=0$ by symmetry. Thus both symmetric and antisymmetric $\mathcal{H}'$ contributions are probably modulated, but no adequate theory is presently available for using $\Delta H(T)$ data to deduce such additional relaxation parameters.

A few approximate calculations[29] of $\omega_{eff}(T)$ for a rigid lattice are available. When short-time or nondiffusive contributions dominate $\psi(T)$, then the temperature dependence[29,30] of the fourth moment $M_4(\beta J_0)$ gives the familiar estimate[3] $\omega_e^2\sim 3M_4/M_2$. Alternatively, spin diffusion occurs even when $\mathcal{H}'=0$, and the temperature dependence[5,31] of the diffusion constant is another estimate for the modulation ω_{eff}, presumably when long-time effects are important. While computations for linear chains are far more complete than for layers, the qualitative features of $\omega_{eff}(T)$ are probably unchanged and can be treated generally for either ferro or antiferromagnetic coupling. The theoretical methods are not entirely consistent, but all lead to small changes of $\lesssim 10\%$ in ω_{eff} over the temperature

range of interest here. We consequently do not expect purely rigid-lattice contributions to account for the residual temperature dependences in Fig. 9.

Thus, the high-T estimate $\omega_{eff} \sim J_0/\hbar$, which can be improved, cannot be safely used to evaluate $|d|$ or $|D|$ on account of probable additional contributions to ΔH. Modulation of $|d|$ or $|D|$ is less important at low T, but there the spin dynamics are not sufficiently well understood to improve on the estimate $\omega_{eff} \sim J_0/\hbar \sim 2 \times 10^5$ G. The value of $d^2/\omega_{eff} \sim 30$ G in Fig. 9 thus leads to $|d| \sim 2.5 \times 10^3$ G ~ 0.25 cm^{-1} in both $PTACuCl_4$ and $PDACuCl_4$. The qualitative values of $|D| \sim 0.10$ cm^{-1} for PTACuCl and $|D| \sim 0.15$ cm^{-1} for $PDACuCl_4$ can be obtained similarly or from the more accurately known ratio $(d/D)^2$ in Fig. 8. More accurate determination of the absolute values of $|d|$ and $|D|$ clearly require systems in which $\omega_{eff}(T)$ can be analyzed.

The temperature dependence of exchange-narrowed EPR lines arising from short-range spin correlations poses general theoretical problems which are only beginning to be resolved. Spin diffusion is important in square-planar antiferromagnetic layers with dipole broadening[23] (e.g., $MnCl_4^{2-}$ salts), but such an approach fails[5] for the one-dimensional antiferromagnet and is qualitatively inconsistent with the behavior of square-planar ferromagnets such as $CuCl_4^{2-}$ salts. It is increasingly evident that different dimensionality, different broadening mechanisms, and different roles of diffusion and of spin correlations must be considered in various systems. While these different special cases are all contained in the general theory, no simple general development is feasible and still further cases will require future examination. The present treatment focuses on antisymmetric and anisotropic exchange in ferromagnetic layers and emphasizes single-crystal techniques for extracting information from the exchange-narrowed absorption.

ACKNOWLEDGMENT

This work was supported by NSF Grant No. GP-CHE76-07377.

*Present address: GCA-Technology Division, Burlington Road, Bedford, Mass. 01730.

†Present address: Office of Safety and Health Administration Laboratory, Salt Lake City, Utah 84109.

[1](a) K. P. Larsen, Acta. Chem. Scand. A 28, 194 (1974); (b) D. N. Anderson and R. D. Willet, Inorg. Chim. Acta. 8, 167 (1974); J. R. Steadman and R. D. Willet, *ibid.* 4, 367 (1970); (c) G. L. Ferguson and B. Zaslow, Acta Crystallogr. B 27, 849 (1971).

[2]L. S. DeJongh and A. R. Miedema, Adv. Phys. 23, 1 (1974); W. E. Hatfield, ACS Symposium Ser. No. 5 (1974) (unpublished).

[3]R. Kubo and T. Tomita, J. Phys. Soc. Jpn. 9, 888 (1954); P. W. Anderson and R. P. Weiss, Rev. Mod. Phys. 25, 269 (1953); A. Abragam, *Principles of Magnetic Resonance* (Oxford U.P., London, 1961), Ch. X.

[4]D. W. Hone and P. M. Richards, Ann. Rev. Mater. Sci. 4, 337 (1974); J. P. Boucher, M. Ahmed Bakheit, M. Nechtschein, M. Villa, G. Bonera, and F. Borsa, Phys. Rev. B 13, 4098 (1976).

[5]P. M. Richards, in *Local Properties at Phase Transitions* (Editrice Compositori, Bologna, Italy, 1975), p. 539.

[6]T. Moriya, Phys. Rev. 120, 91 (1960).

[7]A. Abragam and B. Bleaney, *Electron Paramagnetic Resonances of Transition Ions* (Oxford U.P., New York, 1970), Chap. 9.

[8]M. Date, H. Yamazaki, M. Motokawa, and S. Tazawa, Prog. Theor. Phys. 465, 194 (1970); L. Shia and G. F. Kokoszka, J. Chem. Phys. 60, 1101 (1974); G. F. Kokoszka, in *Low-Dimensional Cooperative Phenomena*, edited by H. J. Keller (Plenum, New York, 1975), p. 171.

[9]K. T. McGregor and Z. G. Soos, J. Chem. Phys. 64, 2506 (1976).

[10]Z. G. Soos, T. T. P. Cheung, and K. T. McGregor, Chem. Phys. Lett. 46, 600 (1977).

[11]D. W. Phelps, D. B. Losee, W. E. Hatfield, and D. J. Hodgson, Inorg. Chem. 15, 3147 (1976).

[12]B. Morosin, P. Fallon, and J. S. Valentine, Acta. Crystallogr. B 31, 2220 (1975).

[13]J. E. Drumheller, D. H. Dickey, R. P. Reklis, C. E. Zaspel, and S. J. Glass, Phys. Rev. B 5, 4631 (1972).

[14]T. G. Castner, Jr., and M. S. Seehra, Phys. Rev. B 4, 38 (1971).

[15]R. D. Willett and M. Extine, Chem. Phys. Lett. 23, 281 (1973).

[16]M. S. Seehra and T. G. Castner, Jr., Phys. Kondens. Mater. 7, 185 (1968).

[17]C. E. Zaspel and J. E. Drumheller, Solid State Commun. 17, 1107 (1975).

[18]R. Kubo, in *Fluctuation, Relaxation, and Resonance in Magnetic Systems*, edited by D. ter Haar (Plenum, New York, 1962).

[19]Z. G. Soos, T. Z. Huang, J. S. Valentine, and R. C. Hughes, Phys. Rev. B 8, 993 (1973).

[20]Z. G. Soos, J. Chem. Phys. 44, 1729 (1966).

[21]R. E. Dietz, F. R. Merritt, R. Dingle, D. Hone, B. G. Silbernagel, and P. M. Richards, Phys. Rev. Lett. 26, 1186 (1971).

[22]F. R. Bartkowski and B. Morosin, Phys. Rev. B 6, 4209 (1972).

[23]P. M. Richards and M. B. Salamon, Phys. Rev. B 9, 32 (1972).

[24]M. J. Hennessy, C. D. McElwee, and P. M. Richards, Phys. Rev. B 7, 930 (1973); T. Z. Huang and Z. G. Soos, *ibid.* 9, 4981 (1974).

[25]R. D. Willett, O. L. Liles, Jr., and C. Michelson, Inorg. Chem. 6, 1185 (1967); B. J. Hathaway and A. A.

G. Tomlinson, Coord. Chem. Rev. 5, 1 (1970).
[26]R. C. Hughes (private communication).
[27]K. T. McGregor and Z. G. Soos, Inorg. Chem. 15, 2159 (1976).
[28]K. T. McGregor and Z. G. Soos (unpublished).
[29]P. M. Richards, Phys. Rev. 142, 196 (1966); M. Tanaker and U. Tomita, Prog. Theor. Phys. 29, 651 (1963).
[30]Y. Tazuke and K. Nagata, J. Phys. Soc. Jpn. 38, 1003 (1975).
[31]F. Mclean and M. Blume, Phys. Rev. B 7, 1149 (1973); J. Hubbard, J. Phys. Soc. Jpn. 39, 1217 (1975).